

## SUPPLEMENTARY INFORMATION

# Multimodality Labeling Strategies for the Investigation of Nanocrystalline Cellulose Biodistribution in a Mouse Model of Breast Cancer

*Mirkka Sarparanta<sup>a,d,\*</sup>, Jacob Pourat<sup>a‡</sup>, Kathryn E. Carnazza<sup>a‡</sup>, Jun Tang<sup>a</sup>, Navid Paknejad<sup>c</sup>,  
Thomas Reiner<sup>a,f</sup>, Mauri A. Kostainen<sup>e</sup> & Jason S. Lewis<sup>a,b,f,g</sup>*

<sup>a</sup>Department of Radiology, <sup>b</sup>Program in Molecular Pharmacology, and <sup>c</sup>Molecular Cytology Core Facility, Memorial Sloan Kettering Cancer Center, New York, New York, USA

<sup>d</sup>Department of Chemistry, Radiochemistry, University of Helsinki, Helsinki, Finland

<sup>e</sup>Biohybrid Materials Group, Department of Bioproducts and Biosystems, Aalto University, Espoo, Finland

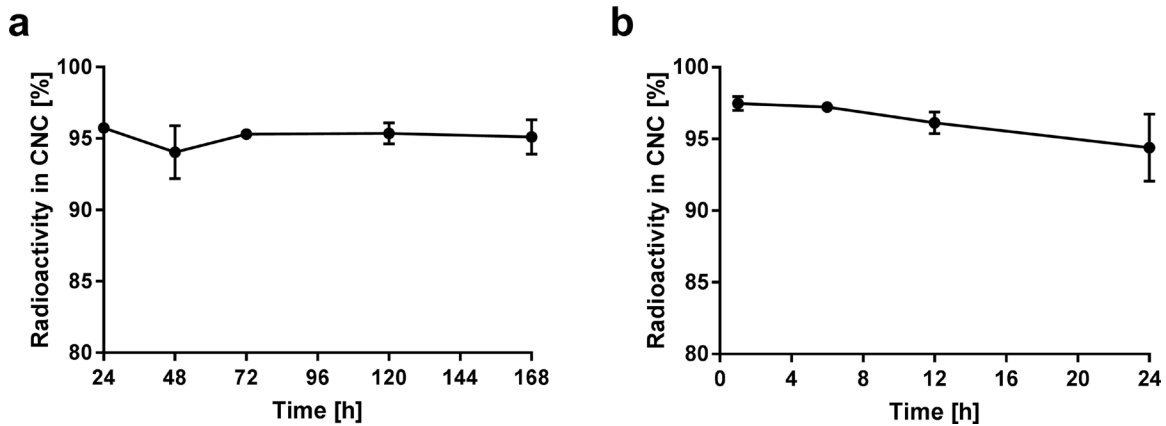
<sup>f</sup>Department of Radiology, and <sup>g</sup>Department of Pharmacology, Weill Cornell Medical College, New York, NY, USA

<sup>‡</sup>These authors contributed equally

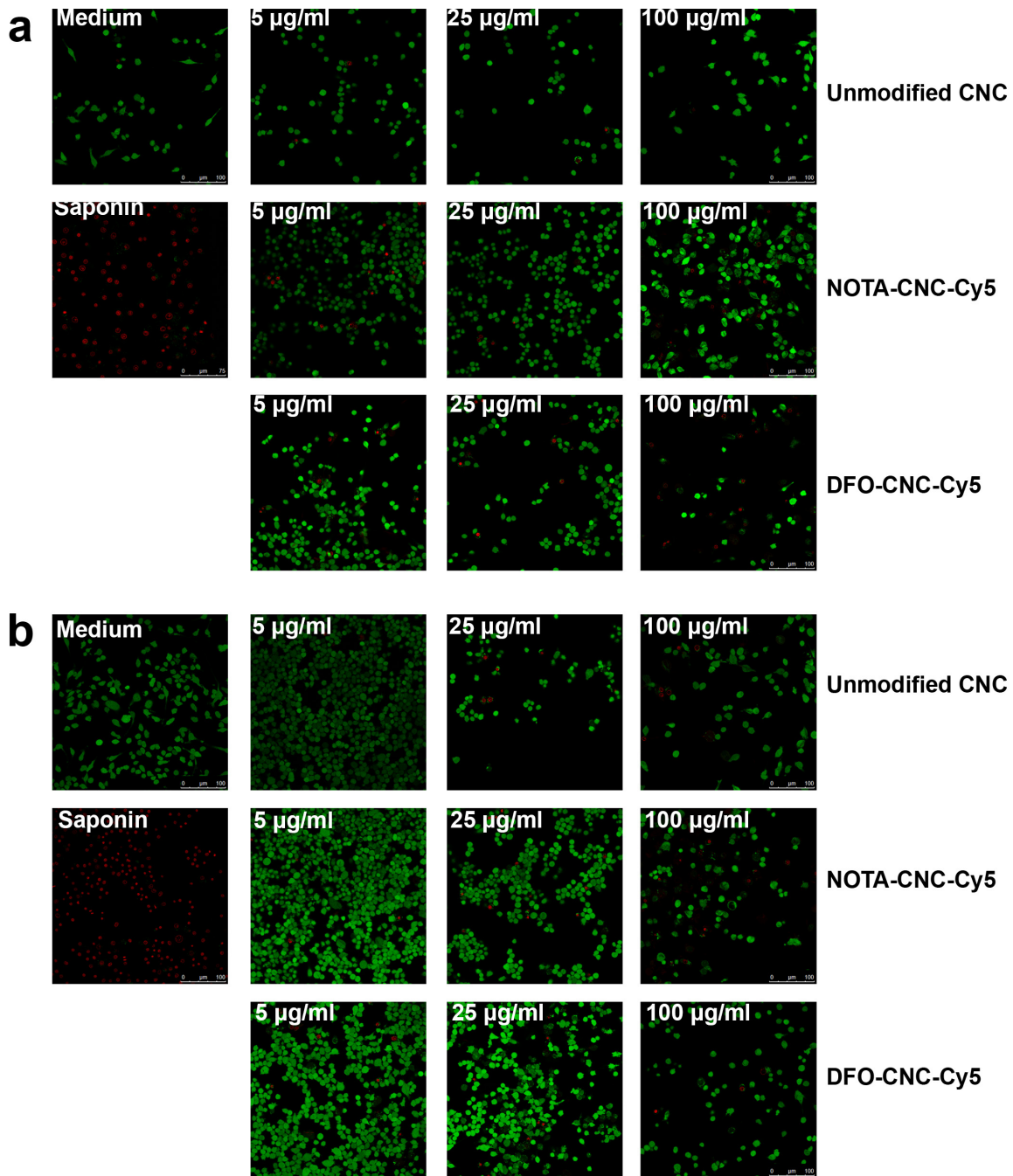
SUPPLEMENTARY INFORMATION TABLE OF CONTENTS

<b>1. Supplementary Figures</b> .....	3
<b>Supplementary Figure S1.</b> .....	3
<b>Supplementary Figure S2.</b> .....	4
<b>Supplementary Figure S3.</b> .....	5
<b>Supplementary Figure S4.</b> .....	6
<b>Supplementary Figure S5.</b> .....	7
<b>Supplementary Figure S6.</b> .....	8
<b>Supplementary Figure S7.</b> .....	9
<b>Supplementary Figure S8.</b> .....	10
<b>Supplementary Figure S9.</b> .....	11
<b>2. Detailed experimental methods</b> .....	12
<i>Surgical procedure for the orthotopic implantation of 4T1 cells</i> .....	12
<i>Generation of control tissue for anti-Cy5 antibody staining</i> .....	12
<i>Immune cell markers and dilutions used for flow cytometry</i> .....	13
<b>Supplementary Table S1.</b> .....	13

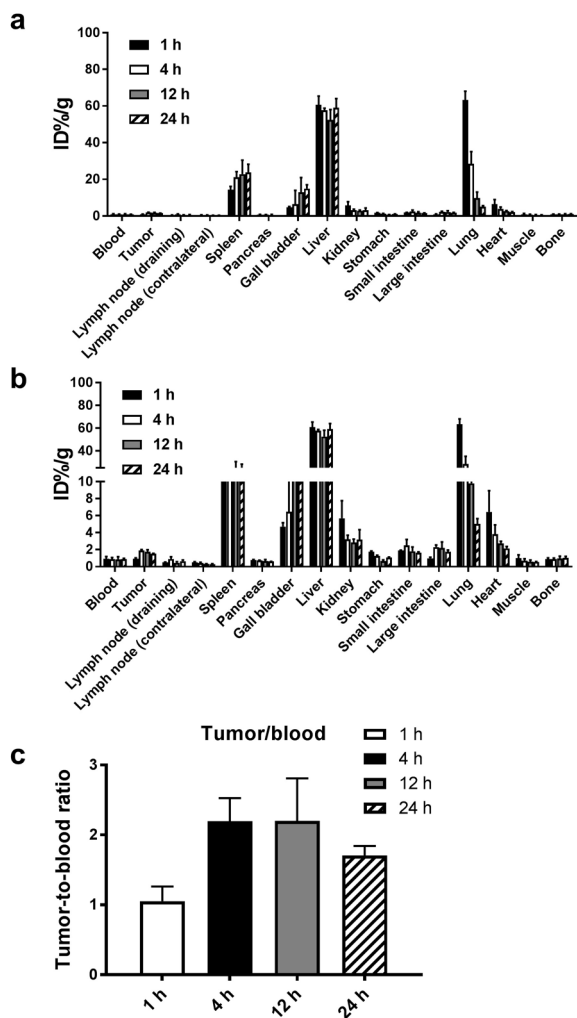
## 1. Supplementary Figures



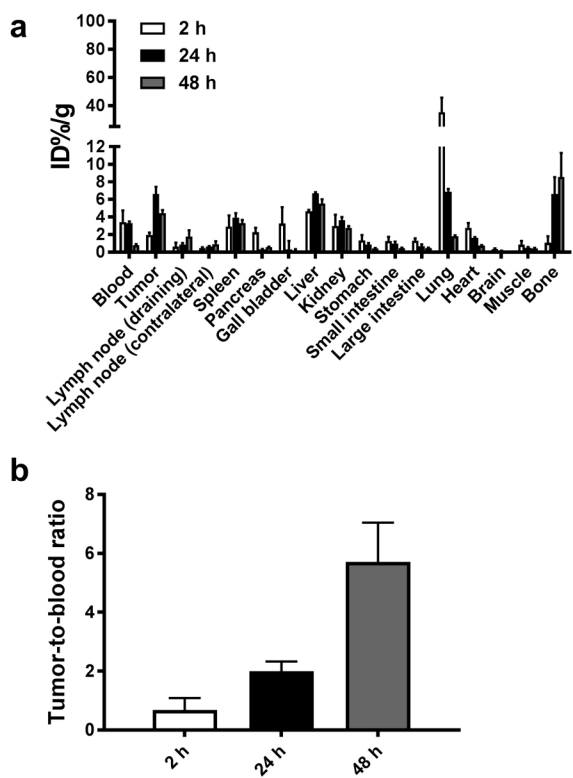
**Supplementary Figure S1.** *In vitro* radiolabel stability of [<sup>89</sup>Zr]Zr-DFO-CNC-Cy5 (a) and [<sup>64</sup>Cu]Cu-NOTA-CNC-Cy5 (b) in human plasma at +37°C. Markers denote mean±SD.



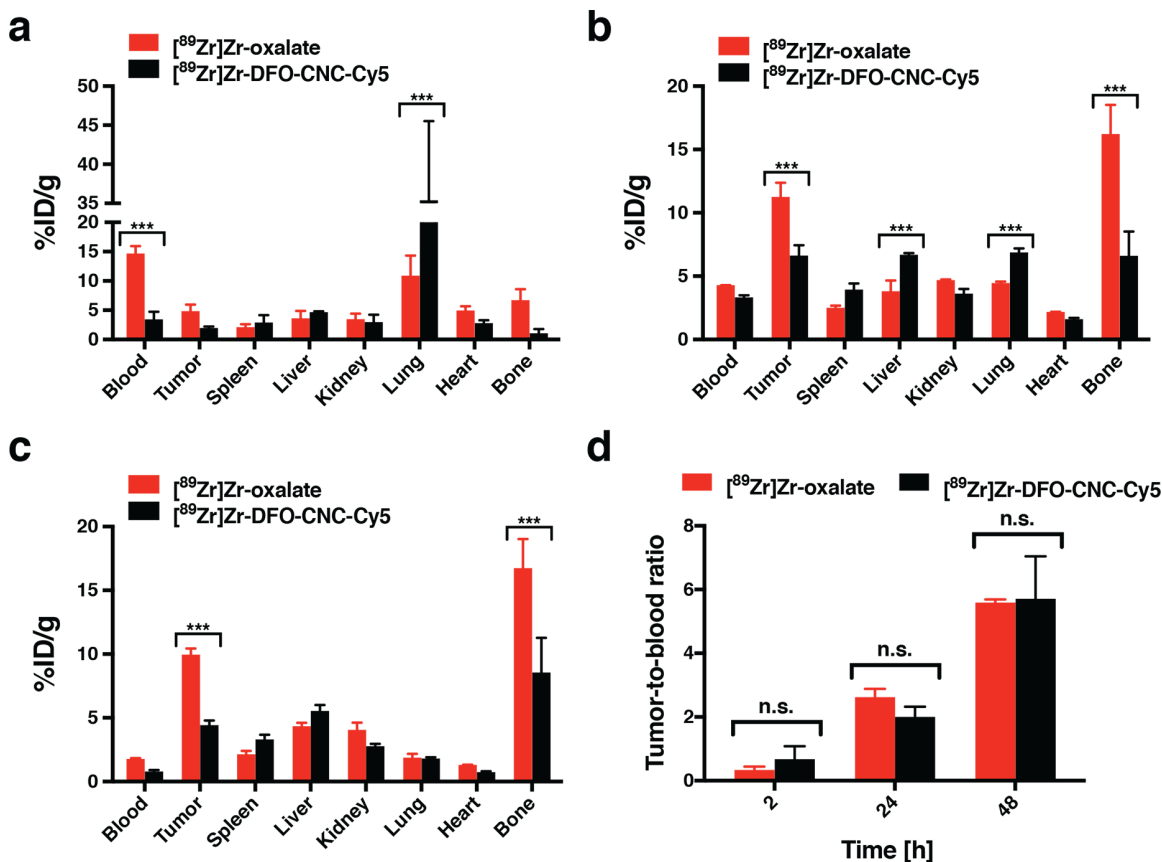
**Supplementary Figure S2.** Representative confocal microscopy images of RAW 264.7 macrophages incubated with different concentrations of unmodified CNC, NOTA-CNC-Cy5, and DFO-CNC-Cy5 for 6 h (a) and 24 h (b). Nuclei of dead cells stain red with EthD-1 after loss of cell membrane integrity, while live cells stain green with Calcein AM due to intracellular esterase activity. Medium and 0.1% saponin are used as controls for live and dead cells, respectively. Scale bar 100  $\mu\text{m}$ .



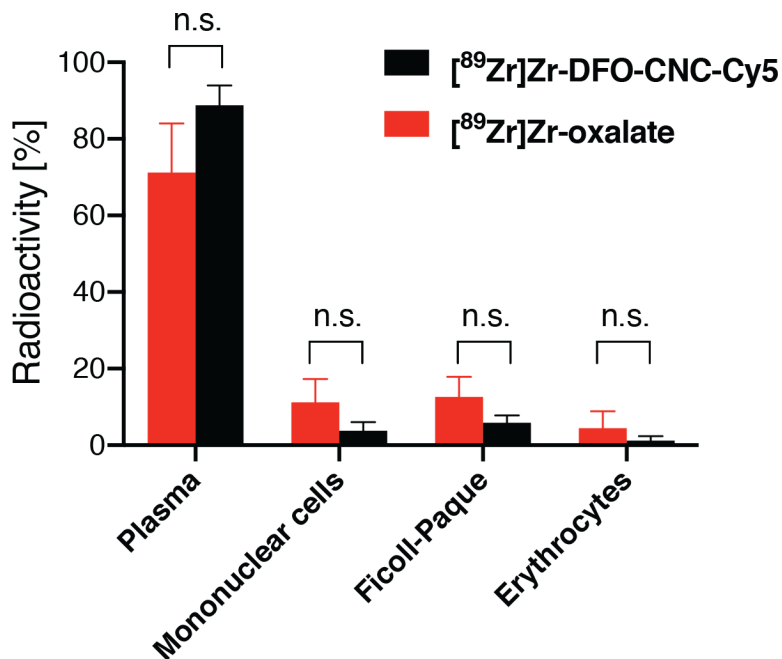
**Supplementary Figure S3.** a) The *ex vivo* biodistribution of  $[^{64}\text{Cu}]\text{Cu-NOTA-CNC-Cy5}$  after single intravenous injection to 4T1-tumor-bearing mice shows rapid accumulation to the liver and spleen, and transient trapping and release in the lung. b) The *ex vivo* biodistribution shown with a cut axis to show data for the organs outside of the reticuloendothelial system (RES). c) The tumor-to-blood ratio for  $[^{64}\text{Cu}]\text{Cu-NOTA-CNC-Cy5}$  at different time points after administration. The ratio peaks at 4 hours, when according to the biodistribution data any circulating nanoparticles have been cleared from the blood stream. Columns represent mean $\pm$ SD ( $n=3$ ) for each time point.



**Supplementary Figure S4.** a) *Ex vivo* biodistribution of  $[^{89}\text{Zr}]\text{Zr-DFO-CNC-Cy5}$  after single intravenous administration to 4T1-tumor-bearing mice shows transient trapping and release of the nanocrystals in the lung, and accumulation of the radioactivity to the tumor peaking at 24 hours after administration. b) The tumor-to-blood ratio for  $[^{89}\text{Zr}]\text{Zr-DFO-CNC-Cy5}$  increases steadily over time. Columns denote mean $\pm$ SD ( $n=3$ ) per time point.

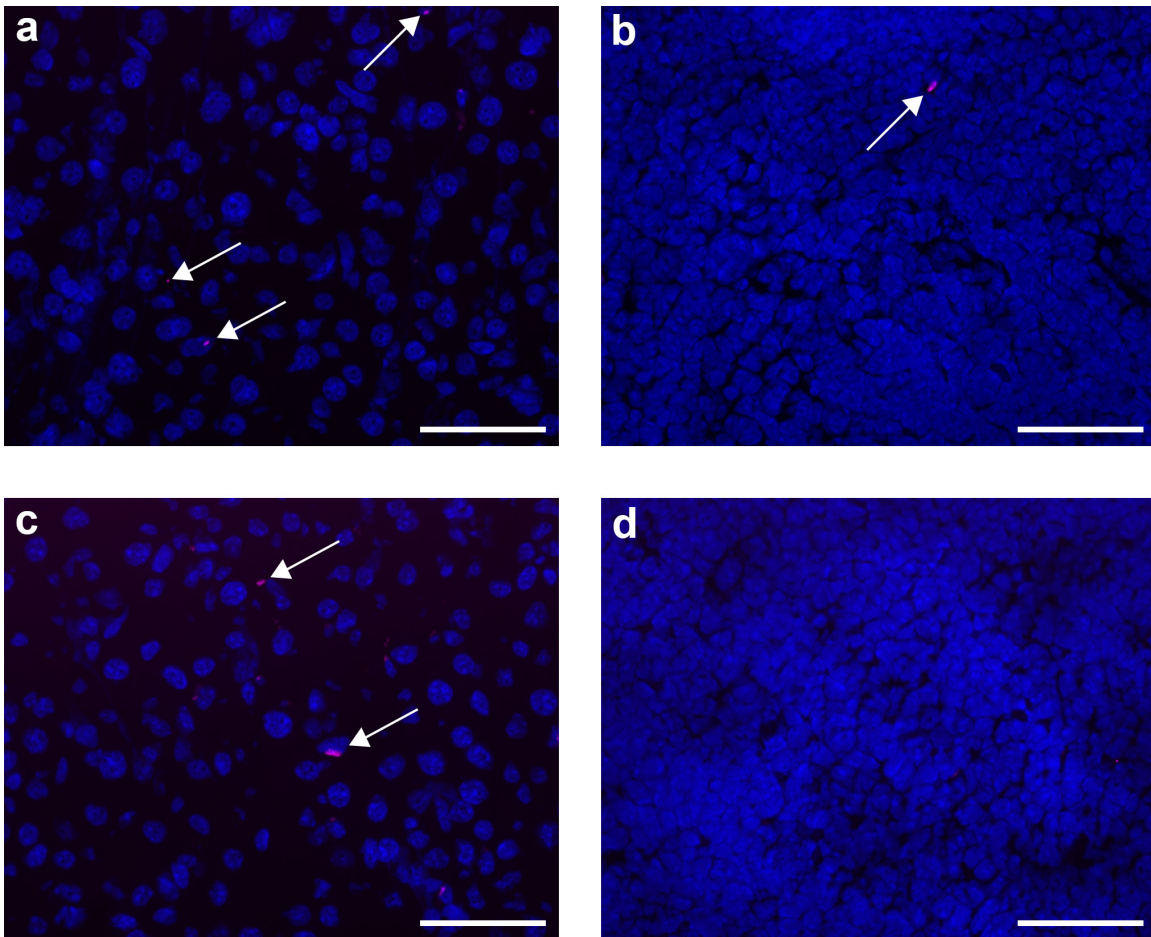


**Supplementary Figure S5.** Comparison of the *ex vivo* biodistribution data for selected tissues between [<sup>89</sup>Zr]Zr-oxalate and [<sup>89</sup>Zr]Zr-DFO-CNC-Cy5 after single intravenous administration to 4T1-tumor-bearing mice at 2 h p.i. (a), 24 h p.i. (b), and 48 h p.i. (c). Comparison of the tumor-to-blood ratios for [<sup>89</sup>Zr]Zr-oxalate and [<sup>89</sup>Zr]Zr-DFO-CNC-Cy5 did not show any significant differences at any time point (d), suggesting that the tumor uptake seen for [<sup>89</sup>Zr]Zr-DFO-CNC-Cy5 can be attributed to a radioactive species other than the intact radiolabeled nanocrystal. Columns denote mean±SD (*n*=3) per time point. Statistical significance was determined using an unpaired *t*-test, with correction for multiple comparisons by the Holm-Sidak method with  $\alpha=0.05$ , and \*\*\**p* < 0.005; ns, non-significant.

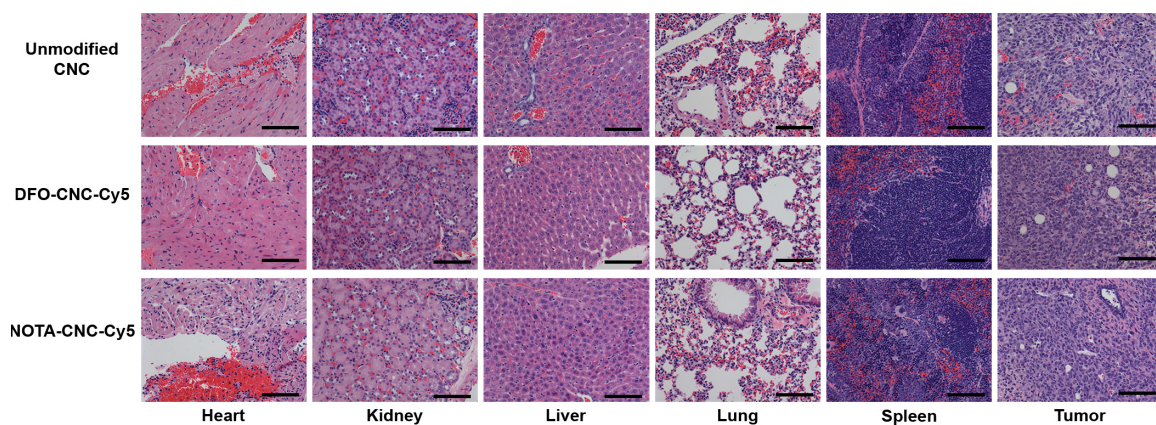


**Supplementary Figure S6.** Comparison of the distribution of radioactivity to the fractionated components of whole mouse blood 4 hours after a single intravenous injection of either [<sup>89</sup>Zr]Zr-oxalate ( $n=4$ ) and [<sup>89</sup>Zr]Zr-DFO-CNC-Cy5 ( $n=3$ ) did not show any significant differences for any of the fractions, further corroborating that the tumor uptake seen for [<sup>89</sup>Zr]Zr-DFO-CNC-Cy5 can be attributed to released <sup>89</sup>Zr in vivo. Columns denote mean $\pm$ SD per fraction. Statistical significance was determined using an unpaired  $t$ -test, with correction for multiple comparisons by the Holm-Sidak method with  $\alpha=0.05$ , and  $***p < 0.005$ ; ns, non-significant.

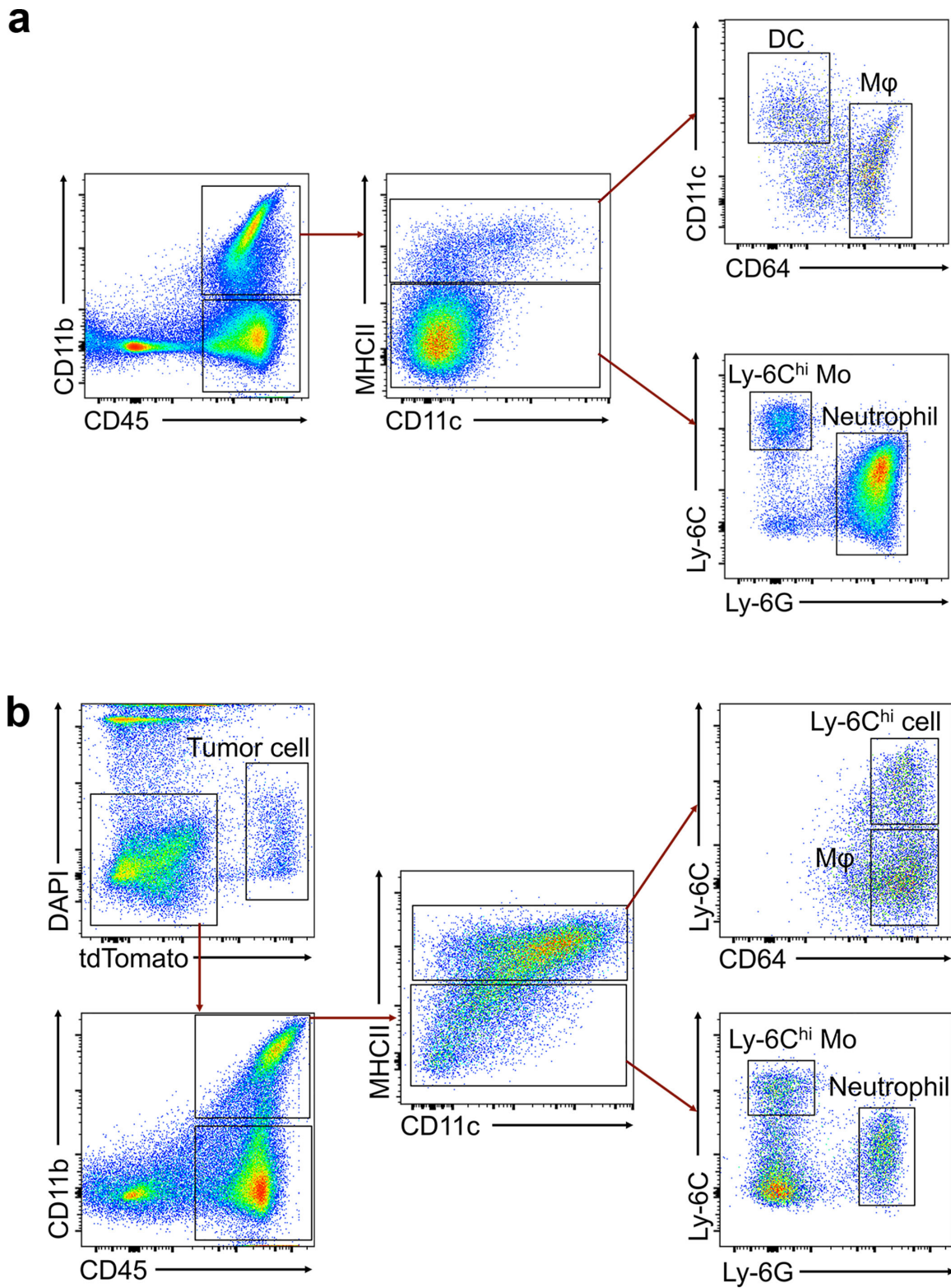




**Supplementary Figure S7.** Fluorescence microscopy of 5- $\mu\text{m}$  cryosections of the liver (a) and spleen (b) of a 4T1-tumor-bearing mouse injected with 25  $\mu\text{g}$  of DFO-CNC-Cy5, and the liver (c) and spleen (d) of an animal receiving 25  $\mu\text{g}$  of NOTA-CNC-Cy5 show only scattered aggregates on the Cy5-labeled CNC (white arrows). Magnification 40 $\times$ , scale bar 50  $\mu\text{m}$ .



**Supplementary Figure S8.** Hematoxylin–eosin (H&E) staining of tissues after systemic delivery of 25  $\mu\text{g}$  of unmodified CNC, DFO-CNC-Cy5, and NOTA-CNC-Cy5 showed no significant differences in the gross histopathology between groups. Magnification 20 $\times$ , scale bar 100  $\mu\text{m}$ .



## 2. Detailed experimental methods

### *Surgical procedure for the orthotopic implantation of 4T1 cells*

Surgical implantation of the 4T1 cells to the right inguinal mammary fat pad of female Balb/c mice was carried out as follows. The mouse was anesthetized with 1–2% isoflurane inhalation (Forane, Baxter Healthcare Corporation, Deerfield, IL, USA) in medical air, and placed supine on the operating area. Meloxicam (2.0 mg/kg in sterile saline) was given subcutaneously, and the animal was placed supine on the operating area. The ventral fur was shaved with electronic clippers, and the surgical area sterilized with alternating scrubs of chlorhexidine–isopropanol and 70% ethanol. The area of the incision was infiltrated with 100  $\mu$ l of 0.5% bupivacaine (Marcaine) in sterile saline. A 5-mm incision was made between the third and fourth teat about 8 mm from the midline, and the mammary fat pad was exteriorized with blunt dissection.  $1 \times 10^6$  4T1 in ice-cold medium were injected in a volume of 50  $\mu$ l using a 27G insulin syringe to the mammary fat pad, which was subsequently returned under the skin. The skin was closed with a single sterile 7-mm AutoClip wound clip (Braintree Scientific, Braintree, MA, USA) and the animal was given warmed sterile saline (10 ml/kg body weight) subcutaneously to facilitate recovery. Wetted food pellets were provided at the bottom of the cage for the first 24 hours post-operatively. Animals received meloxicam 2.0 mg/kg subcutaneously also 24 hours after surgery. Wound clips were removed on day 7 following surgery.

### *Fractionation of whole blood for determination of radioactivity distribution between the blood components*

Four hours after intravenous injection of either 0.3 MBq of [ $^{89}\text{Zr}$ ]Zr-DFO-CNC-Cy5 or 0.3 MBq of [ $^{89}\text{Zr}$ ]Zr-oxalate in 0.5% Kolliphor HS 15–1 $\times$ PBS, pH=7.4 to female Balb/c mice (6 weeks, Janvier Labs, Saint Berthevin, France), whole blood (0.5 ml) was collected by cardiac puncture after CO<sub>2</sub> asphyxiation and diluted with 0.5 ml of 100 IU heparin in 1 $\times$ PBS. The diluted blood sample was overlaid to 0.75 ml of Ficoll-Paque PLUS density gradient medium (GE Healthcare, density 1.077 g ml<sup>-1</sup>) in a 2.0-ml Protein LoBind microtube (Eppendorf) and separated by centrifugation at 400g for 35 minutes (22°C). The plasma, peripheral mononuclear cells, Ficoll-Paque medium and erythrocyte fractions were separated to 5-ml polystyrene tubes and their radioactivity counted on an automated gamma counter (Wizard 3", PerkinElmer, Turku, Finland) with a 5-minute counting time.

### *Generation of control tissue for anti-Cy5 antibody staining*

Female outbred nu/nu mice (aged 6–8 weeks, Charles River) were implanted with a 60-day-release 17 $\beta$ -estradiol pellet (0.72 mg, Innovative Research of America, Sarasota, FL, USA) using aseptic technique under isoflurane anesthesia. Six days following the implantation of the 17 $\beta$ -estradiol pellet,  $10 \times 10^6$  BT-474 cells were implanted in the right flank, and the tumors were allowed to grow for 5 weeks until a diameter of 8 mm in the largest dimension was reached. Trastuzumab (Herceptin) injection from a multidose vial was purified from formulation additives with sequential passages through a PD-10 size

exclusion column (GE Healthcare), and a 50-kDa MWCO ultrafiltration device (Amicon, Merck Millipore Corporation). Human IgG was purchased from Sigma-Aldrich Corporation, and used as supplied. 2.0 mg of both trastuzumab and human IgG were labeled with Cy5 using a Cy5<sup>®</sup> Fast Conjugation Kit based on EDC/NHS coupling chemistry (Abcam) according to the manufacturer’s instructions. The Cy5-labeled antibodies were purified by size exclusion chromatography on a PD-10, and formulated in 1% BSA–1×PBS, pH=7.4, and stored at +4°C until use. The immunoreactivity of the labeled antibodies was confirmed in BT-474 cells with fluorescence microscopy before the in vivo experiment. BT-474 tumor-bearing mice (*n*=2 per group) were intravenously injected with 20 µg of either Cy5-trastuzumab or Cy5-IgG, and sacrificed 72 hours later by CO<sub>2</sub> asphyxiation followed by cervical dislocation. The tumor was dissected, fixed in 10% neutral buffered formalin, embedded in paraffin, sectioned, and processed for the anti-Cy5 IHC staining alongside the CNC samples.

*Immune cell markers and dilutions used for flow cytometry*

The following immune cell markers and respective fluorescent dyes were used in the immune cell flow cytometry experiment. All antibodies were purchased readily conjugated from BD Biosciences (San Jose, CA, USA) or BioLegend (San Diego, CA, USA). Single-cell suspensions of 4T1-tdTomato tumors and spleen from animals receiving either NOTA-CNC-Cy5, DFO-CNC-Cy5, or PBS were diluted to 10×10<sup>6</sup> cells/ml and applied to a 96-well plate at a concentration of 2×10<sup>6</sup> cells/well. The antibody cocktail was prepared according to the dilutions below to a volume of 100 µl/well in FACS buffer (DPBS with 1% FBS, 0.5% BSA, 0.1% NaN<sub>3</sub>, and 1 mM EDTA). DAPI was added to the final flow cytometry samples at a concentration of 1:100.

Channel	1	2	3	4	5	6	7	8	9	10
Dye	DAPI	BV510	FITC	BV605	tdTomato	Cy5	PE-Cy7	APC-Cy7	BV711	BV786
Marker	Viability	CD45	CD64	CD11b	Tumor	CNC	CD11c	Ly6C	Ly6G	MHCII
Dilution	1:100*	1:200	1:200	1:200	N/A	N/A	1:200	1:400	1:400	1:400

**Supplementary Table S1.** Fluorescent dyes and markers used in the immune cell flow cytometry experiment. \*Applied to the final flow cytometry sample.